JOC Article

pubs.acs.org/joc

Bisnicalaterines B and C, Atropisomeric Bisindole Alkaloids from *Hunteria zeylanica*, Showing Vasorelaxant Activity

Yusuke Hirasawa,[†] Mayumi Hara,[†] Alfarius E. Nugroho,[†] Masatomo Sugai,[†] Kazumasa Zaima,[†] Nobuo Kawahara,[‡] Yukihiro Goda,[‡] Khalijah Awang,[§] A. Hamid A. Hadi,[§] Marc Litaudon,[⊥] and Hiroshi Morita*,[†]

[†]*Faculty of Pharmaceutical Sciences, Hoshi University, Shinagawa-ku, Tokyo 142-8501, Japan,* [‡]*National Institute of Health Sciences, Kamiyoga 1-18-1, Setagaya-ku, Tokyo 158-8501, Japan,* [§]*Department of Chemistry, Faculty of Science, University of Malaya, 50603 Kuala Lumpur, Malaysia, and* [⊥]*Institut de Chimie de la Substances Naturelles, Centre Nationale de la Recherches Scientifique, 91198, Gif-sur Yvette, Cedex, France*

moritah@hoshi.ac.jp

Received April 9, 2010

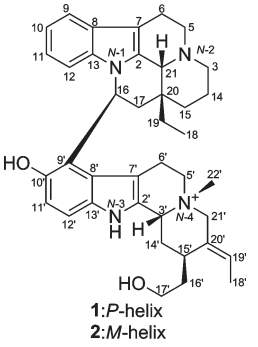

Two new bisindole alkaloids, bisnicalaterines B and C (**1** and **2**) consisting of an eburnane and a corynanthe type of skeletons, were isolated from the bark of *Hunteria zeylanica*. Their absolute structures were determined by combination of NMR, CD, and computational methods, and each of them was shown to be in an atropisomeric relationship. Bisnicalaterines B and C (**1** and **2**) showed potent vasorelaxant activity on isolated rat aorta.

Introduction

Hunteria zeylanica (Retz.) Gardner ex Thwaites is a member of the Apocynaceae family in Malaysia, found mostly in Pahang and Selangor.[1] Traditionally, the latex has been used for smearing on the sores caused by yaws.[2] The bark and leaves have been known to produce various skeletal alkaloids depending on the area where the plants were distributed.[3−8] Some pharmacological actions such as antinociceptive, antipyretic, and anti-inflammatory activities have also been reported.[9−15] In our previous paper,[16] we have reported the isolation of a new bisindole alkaloid,

(1) Whitmore, T. C. *Tree Flora Malaysia*; Longman: FRIM, 1973.
(2) Perry, L. M. *Medicinal Plants of East and Southeast Asia: Attributed Properties and Uses*; The MIT Press: Cambridge, MA, 1980.
(3) Lavaud, C.; Massiot, G.; Vercauteren, J.; Le Menolivier, L. *Phytochemistry* **1982**, *21*, 445–447.
(4) Subhadhirasakul, S.; Aimi, N.; Takayama, H.; Ponglux, D.; Sakai, S. *Chem. Pharm. Bull.* **1994**, *42*, 991–993.
(5) Subhadhirasakul, S.; Takayama, H.; Miyabe, Y.; Kitajima, M.; Ponglux, D.; Sakai, S.; Aimi, N. *Heterocycles* **1995**, *41*, 2049–2056.
(6) Subhadhirasakul, S.; Takayama, H.; Miyabe, Y.; Aimi, N.; Ponglux, D.; Sakai, S. *Chem. Pharm. Bull.* **1994**, *42*, 2645–2646.
(7) Takayama, H.; Subhadhirasakul, S.; Mizuki, J.; Kitajima, M.; Aimi, N.; Ponglux, D.; Sakai, S. *Chem. Pharm. Bull.* **1994**, *42*, 1957–1959.
(8) Takayama, H.; Subhadhirasakul, S.; Ohmori, O.; Kitajima, M.; Ponglux, D.; Aimi, N. *Heterocyles* **1998**, *47*, 87–90.
(9) Leewanich, P.; Tohda, M.; Matsumoto, K.; Subhadhirasakul, S.; Takayama, H.; Aimi, N.; Watanabe, H. *Eur. J. Pharmacol.* **1997**, *332*, 321–326.
(10) Leewanich, P.; Tohda, M.; Matsumoto, K.; Subhadhirasakul, S.; Takayama, H.; Aimi, N.; Watanabe, H. *Eur. J. Pharmacol.* **1998**, *348*, 271–277.
(11) Leewanich, P.; Tohda, M.; Matsumoto, K.; Subhadhirasakul, S.; Takayama, H.; Watanabe, H. *Biol. Pharm. Bull.* **1996**, *19*, 394–399.
(12) Reanmongkol, W.; Matsumoto, K.; Watanabe, H.; Subhadhirasakul, S.; Sakai, S. *Biol. Pharm. Bull.* **1994**, *17*, 1345–1350.
(13) Reanmongkol, W.; Tohda, M.; Matsumoto, K.; Subhadhirasakul, S.; Takayama, H.; Sakai, S.; Watanabe, H. *Biol. Pharm. Bull.* **1995**, *18*, 910–912.
(14) Reanmongkol, W.; Matsumoto, K.; Watanabe, H.; Subhadhirasakul, S.; Takayama, H.; Sakai, S. *Biol. Pharm. Bull.* **1995**, *18*, 33–36.
(15) Mohamad, K.; Suzuki, T.; Baba, Y.; Zaima, K.; Matsuno, Y.; Hirasawa, Y.; Mukhtar, M. R.; Awang, K.; Hadi, A. H. A.; Morita, H. *Heterocycles* **2007**, *74*, 969–976.
(16) Nugroho, A. E.; Hirasawa, Y.; Kawahara, N.; Goda, Y.; Awang, K.; Hadi, A. H. A.; Morita, H. *J. Nat. Prod.* **2009**, *72*, 1502–1506.

Published on Web 05/14/2010 DOI: 10.1021/jo1006762

TABLE 1. ^{1}H and ^{13}C NMR Data of Bisnicalaterines B and C (**1** and **2**) in CD_3OD at 300 K[a]

	1		**2**	
position	δ_H (J, Hz)	δ_C	δ_H (J, Hz)	δ_C
2		127.4		127.1
3a	3.13 (1H, m)	46.1	3.05 (1H, dd, 12.0, 12.0)	45.9
3b	3.30 (1H, m)		3.26 (1H, m)	
5a	3.82 (1H, m)	52.4	3.77 (1H, m)	52.3
5b	3.92 (1H, m)		3.89 (1H, m)	
6a	3.18 (1H, m)	17.0	3.18 (1H, m)	17.1
6b	3.18 (1H, m)		3.18 (1H, m)	
7		105.6		103.1
8		128.4		128.0
9	7.48 (1H, brd, 6.5)	119.3	7.44 (1H, d, 7.7)	119.2
10	6.96 (1H, m)	121.2	6.97 (1H, dd, 7.7, 7.5)	120.6
11	6.74 (1H, t, 7.6)	123.2	6.76 (1H, dd, 7.9, 7.5)	122.7
12	6.33 (1H, d, 7.6)	113.2	6.56 (1H, d, 7.9)	111.9
13		138.7		138.4
14a	1.76 (1H, m)	19.4	1.75 (1H, m)	19.4
14b	2.03 (1H, m)		2.03 (1H, m)	
15a	1.56 (1H, dd, 11.6, 11.6)	23.2	1.49 (1H, dd, 11.3, 11.3)	23.7
15b	1.74 (1H, m)		1.72 (1H, m)	
16	6.14 (1H, d, 8.6)	49.7	5.86 (1H, dd, 11.5, 5.5)	50.9
17a	2.08 (1H, m)	40.8	2.32 (1H, dd, 14.1, 5.5)	38.4
17b	2.39 (1H, m)		2.74 (1H, dd, 14.1, 11.5)	
18	0.98 (3H, m)	7.3	1.02 (3H, t, 7.1)	7.4
19a	1.65 (1H, m)	28.7	1.69 (1H, m)	28.8
19b	2.14 (1H, m)		2.06 (1H, m)	
20		37.1		36.6
21	4.99 (1H, m)	61.9	4.89 (1H, m)	61.6
2′		131.3		132.1
3′	4.62 (1H, brd, 10.0)	62.4	4.93 (1H, m)	62.9
5′a	2.83 (1H, m)	52.4	3.32 (1H, m)	52.4
5′b	3.62 (1H, m)		4.07 (1H, ddd, 11.0, 11.0, 5.2)	
6′a	0.86 (1H, m)	21.2	3.37 (1H, m)	21.9
6′b	2.71 (1H, brd, 14.8)		3.48 (1H, m)	
7′		102.0		101.5
8′		124.9		125.9
9′		117.9		117.6
10′		149.3		151.1
11′	6.93 (1H, m)	113.6	7.21 (1H, d, 8.4)	113.0
12′	7.28 (1H, brd, 7.2)	113.3	6.66 (1H, d, 8.4)	115.0
13′		134.1		133.2
14′a	2.09 (1H, m)	36.1	2.41 (1H, m)	36.8
14′b	2.25 (1H, m)		2.41 (1H, m)	
15′	3.13 (1H, m)	30.3	3.26 (1H, m)	30.5
16′a	1.84 (1H, m)	34.4	1.95 (1H, m)	34.6
16′b	1.94 (1H, m)		2.08 (1H, m)	
17′a	3.50 (1H, m)	60.0	3.59 (1H, m)	60.2
17′b	3.61 (1H, m)		3.70 (1H, m)	
18′	1.72 (3H, m)	13.2	1.78 (3H, d, 6.7)	13.4
19′	5.77 (1H, m)	131.7	5.90 (1H, q, 6.7)	132.1
20′		129.2		129.4
21′a	3.61 (1H, m)	67.8	3.95 (1H, d, 13.3)	68.2
21′b	4.14 (1H, brd, 12.4)		4.40 (1H, d, 13.3)	
22′	2.41 (3H, s)	48.3	3.26 (3H, s)	50.0

[a] δ in ppm.

bisnicalaterine A, consisting of two vobasine-type skeletons from the leaves of *H. zeylanica*. Recently, we have reported that some alkaloids such as cassiarin A from *Cassia siamea* and alstilobanine A from *Alstonia angustiloba* showed a vasorelaxant effect on rat aorta.[17] In our search for bioactive alkaloids targeting aortic smooth muscle from medicinal

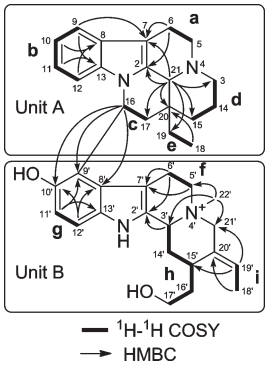

FIGURE 1. Selected 2D NMR correlations for bisnicalaterine B (**1**).

plants, bisnicalaterine B (**1**) and its atropisomeric bisnicalaterine C (**2**), two new bisindole alkaloids consisting of an eburnane and a corynanthe type of skeletons, have been isolated from the bark of *H. zeylanica,* both of which showed vasorelaxant effect on rat aorta. In this paper, we describe the isolation and structure elucidation of **1** and **2** and its vasorelaxant effect on rat aorta.

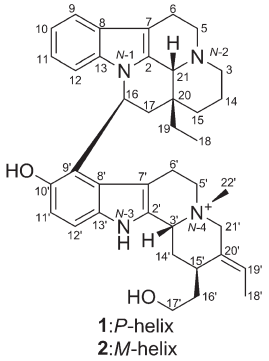

Results and Discussion

Structure of Bisnicalaterine B (1). Bisnicalaterine B (**1**) showed the molecular formula $C_{39}H_{49}N_4O_2$, which was determined by HRESIMS [m/z 605.3878 $(M)^+$, Δ +2.2 mmu]. The IR absorption band was characteristic of an amino or hydroxyl (3430 cm^{-1}) group. ^{1}H and ^{13}C NMR data (Table 1) suggested the presence of one sp^3 quaternary carbon, 13 sp^3 methylenes, four sp^3 methines, three methyls, seven sp^2 methines, and 11 sp^2 quaternary carbons. Among them, four sp^3 methylenes (δ_C 46.1; δ_H 3.13 and 3.30, δ_C 52.4; δ_H 3.82 and 3.92, δ_C 52.4; δ_H 2.83 and 3.62, and δ_C 67.8; δ_H 3.61 and 4.14), three sp^3 methines (δ_C 49.7; δ_H 6.14, δ_C 61.9; δ_H 4.99, and δ_C 62.4; δ_H 4.62), one methyl (δ_C 48.3; δ_H 2.41), and four sp^2 quaternary carbons (δ_C 127.4, δ_C 131.3, δ_C 134.1, and δ_C 138.7) were attached to the nitrogen atom.

The gross structure of **1** was deduced from extensive analyses of the two-dimensional NMR data, including the $^{1}H-^{1}H$ COSY, HMQC, and HMBC spectra in CD_3OD (Figure 1). The $^{1}H-^{1}H$ COSY and HMQC spectra revealed

(17) (a) Morita, H.; Tomizawa, Y.; Deguchi, J.; Ishikawa, T.; Arai, H.; Zaima, K.; Hosoya, T.; Hirasawa, Y.; Matsumoto, T.; Kamata, K.; Ekasari, W.; Widyawaruyanti, A.; Wahyuni, T. S.; Zaini, N. C.; Honda, T. *Bioorg. Med. Chem.* **2009**, *17*, 8234–8240. (b) Koyama, K.; Hirasawa, Y.; Zaima, K.; Hoe, T. C.; Chan, K.-L.; Morita, H. *Bioorg. Med. Chem.* **2008**, *16*, 6483–6488.

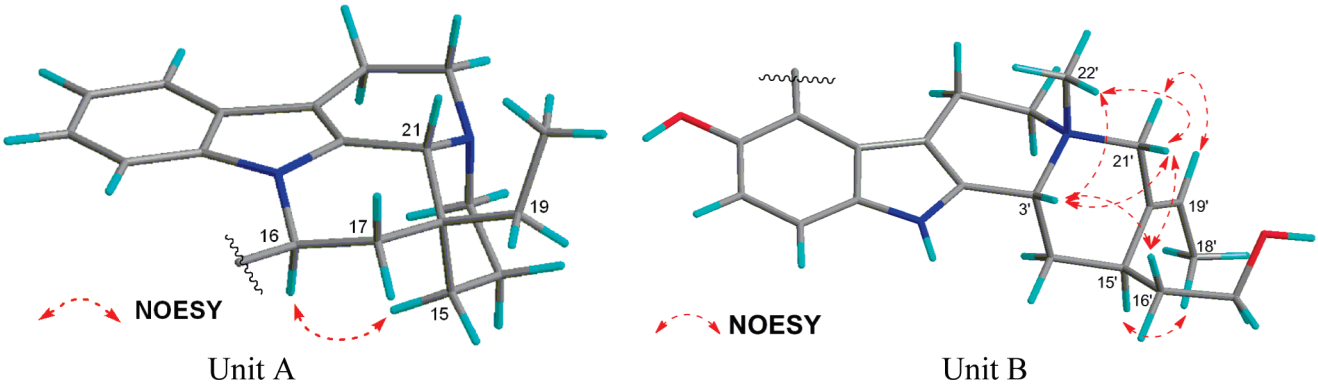

FIGURE 2. Selected NOESY correlations for units A and B in bisnicalaterine B (**1**).

connectivities of nine partial structures **a** (C-5−C-6), **b** (C-9−C-12), **c** (C-16−C-17), **d** (C-3, C-14−C-15), **e** (C-18−C-19), **f** (C-5′−C-6′), **g** (C-11′−C-12′), **h** (C-3′, C-14′−C-17′), and **i** (C-18′−C-19′) as shown in Figure 1. These partial structures were classified into two units A and B.

In unit A, the connectivity of partial structure **a** and indole ring (C-2, C-7−C-13 and N-1) was revealed by the HMBC correlations of H-9 and H-6 to C-7 (δ_C 105.6) and H-6 to C-2 (δ_C 127.4). HMBC correlations from H-21 to C-7, C-15 (δ_C 23.2), C-17 (δ_C 40.8), C-19 (δ_C 28.7), and C-20 (δ_C 37.1) established the connections among C-15, C-17, C-19, and C-21 through C-20 and connection between C-21 and C-2. HMBC cross peaks of H-21 to C-3 (δ_C 46.1) suggested the linkage between C-3 and C-21 through a nitrogen atom. The ^{1}H and ^{13}C NMR chemical shifts of C-5 (δ_C 52.4; δ_H 3.82 and 3.92) and C-16 (δ_C 49.7; δ_H 6.14) were characteristic of an eburnane skeleton.[18]

In unit B, the presence of an indole ring (C-2′, C-7′−C-13′) was revealed by the HMBC correlations of H-6′ to C-2′ (δ_C 131.3) and C-7′ (δ_C 102.0), H-11′ to C-9′ (δ_C 117.9) and C-13′ (δ_C 134.1), H-12′ to C-8′ (δ_C 124.9) and C-10′ (δ_C 149.3). HMBC cross-peaks of H_3-22′ to C-3′, C-5′, and C-21′ established the connections among C-3′, C-5′, C-21′, and C-22′ through N-4′. The connectivity of C-2′ and C-3′ was deduced by HMBC correlation of H-3′ to C-2. The presence of an ethylidene group at C-20′ was indicated by HMBC correlations of H_3-18′ to C-20′ and H-19′ to C-15′ and C-21′. Detailed analyses of the ^{13}C chemical shifts (δ_C 149.3 and δ_C 60.0) of C-10′ and C-17′ indicated they were attached to an oxygen atom. These data implied unit B possessed a corynanthe skeleton. Finally, the linkage between units A at C-16 and B at C-9′ was provided by HMBC correlations of H-16 to C-8′, C-9′, and C-10′. Thus, the gross structure of bisnicalaterine B (**1**) was assigned to be a new bisindole alkaloid connecting between C-16 of an eburnane and C-9′ of a corynanthe skeletons as shown in Figure 1.

Stereochemistry of Bisnicalaterine B (1). The stereochemistry of each monoterpeneindole unit in **1** was assigned by NOESY correlations as shown in the computer-generated 3D drawing (Figure 2). In unit A, the NOESY correlations of H-15a/H-16 suggested that C-15 and H-16 were α-oriented and H-21 and an ethyl group (C-18−C-19) were β-oriented, respectively. While in unit B, the NOESY correlations of H-3′/H_3-22′, H-21′a, and H-16′a, H_3-22′/H-21′a, and H-21′a/H-16′a suggested that H-3′, C-16′, and C-22′ were β-oriented, while the correlations of H-19′/H-21′b and H-15′/H_3-18′ established the *E*-configuration of the ethylidene side chain. Thus, the relative stereochemistry of units A and B was assigned as shown in Figure 2.

Finally, the conformation of **1** through the C-16−C-9′ bond was assigned by the NOESY correlations of H-6′b/H-17a and by the highly shifted chemical shifts (δ_H 0.86 and 2.41) of H-6′a and Me-22′ at an ammonium nitrogen atom, which can be explained by the anisotropic effect of the indole ring as shown in the computer-generated 3D drawing (Figure 3).

Structure and Stereochemistry of Bisnicalaterine C (2). Bisnicalaterine C (**2**) showed the molecular formula $C_{39}H_{49}N_4O_2$, which was determined by HRESIMS [*m*/*z* 605.3814 $(M)^+$, Δ −4.2 mmu]. The IR absorption band was characteristic of an amino or hydroxyl (3430 cm^{-1}) group. ^{1}H and ^{13}C NMR data (Table 1) suggested the presence of one sp^3 quaternary carbons, 13 sp^3 methylenes, four sp^3 methines, three methyls, seven sp^2 methines, and 11 sp^2 quaternary carbons.

The molecular weight and the ^{1}H and ^{13}C NMR data suggested that bisnicalaterine C (**2**) was an isomer of bisnicalaterine B (**1**). Further analysis of the two-dimensional NMR data (^{1}H−^{1}H COSY, HMQC, and HMBC spectra in CD_3OD) of **2** revealed the same planar structure as in **1**. Analysis of the NOESY spectral data also suggested that **2** had the same configuration as in **1** for both unit A and unit B. The only noticeable difference in NOESY correlations of **1** and **2** is the correlations between unit A and unit B as follows. The H-6′b/H-16 correlation was observed in **2** instead of the H-6′b/H-17a correlation as observed in **1**. The correlation of H-6′b/H-16 was used to assign the conformation of **2** through the C-16−C-9′ bond as shown in Figure 3.

Theoretical calculation of the total molecular energy as a function of the dihedral angle N_1−C_{16}−$C_{9'}$−$C_{10'}$ showed two

(18) Gan, C. Y.; Robinson, W. T.; Etoh, T.; Hayashi, T.; Komiyama, K.; Kam, T. S. *Org. Lett.* **2009**, *11*, 3962–3965.
(19) Muller, J. M.; Davis, M. J.; Kuo, L.; Chilian, W. M. *Am. J. Physiol.* **1999**, *276*, H1706–H1714.
(20) Muller, B.; Kleschyov, A. V.; Gyorgy, K.; Stoclet, J. C. *Physiol. Res.* **2000**, *49*, 19–26.
(21) Faraci, F. M.; Heistad, D. D. *Physiol. Rev.* **1998**, *78*, 53–97.
(22) Standen, N. B.; Quayle, J. M. *Acta. Physiol. Scand.* **1998**, *164*, 549–577.
(23) Tanaka, Y.; Koike, K.; Toro, L. *J. Smooth Muscle Res.* **2004**, *40*, 125–153.
(24) Shieh, C. C.; Coghlan, M.; Sullivan, J. P.; Gopalakrishnan, M. *Pharmacol. Rev.* **2000**, *52*, 557–594.
(25) Dias, K. L.; Correia, Nde. A.; Pereira, K. K.; Barbosa-Filho, J. M.; Cavalcante, K. V.; Araujo, I.G.l; Silva, D. F.; Guedes, D. N.; Neto, M. A.; Bendhack, L. M.; Medeiros, I. A. *Eur. J. Pharmacol.* **2007**, *574*, 172–178.

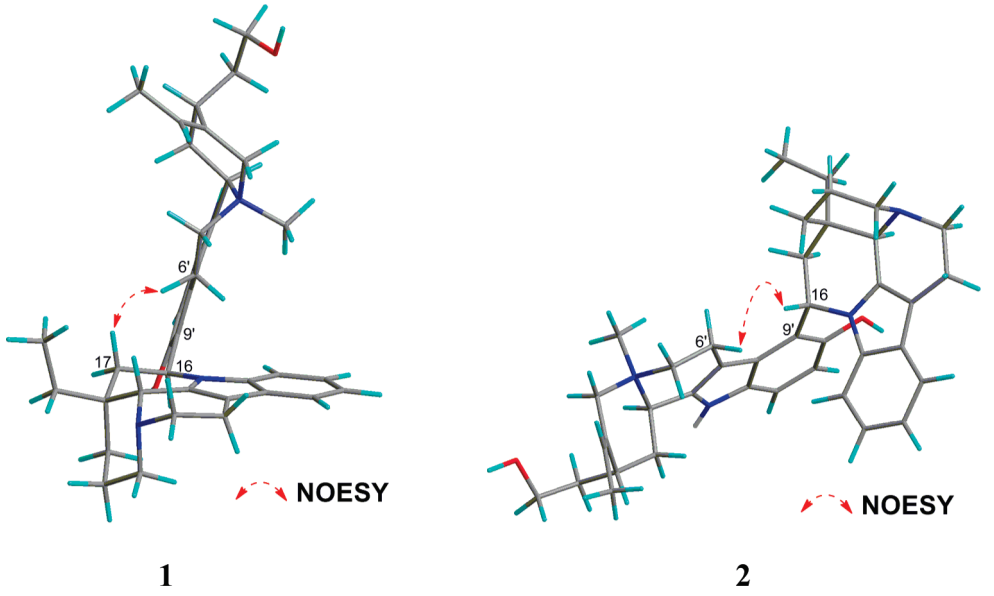

FIGURE 3. Stereostructures of bisnicalaterines B and C (**1** and **2**) with selected NOESY correlations.

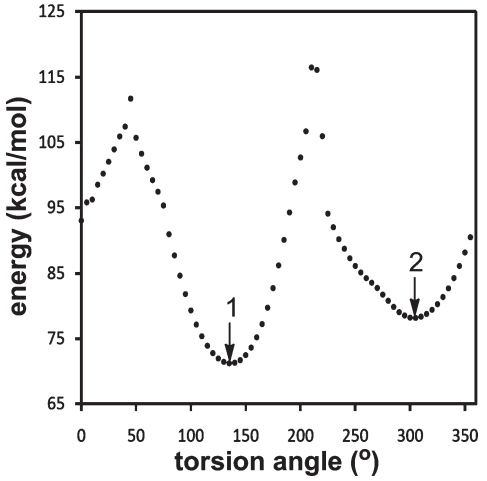

FIGURE 4. Energy and torsion angle contour plot of bisnicalaterines B (**1**) and C (**2**) by Grid search. Each conformer corresponding to each energy minima was shown in Figure 3.

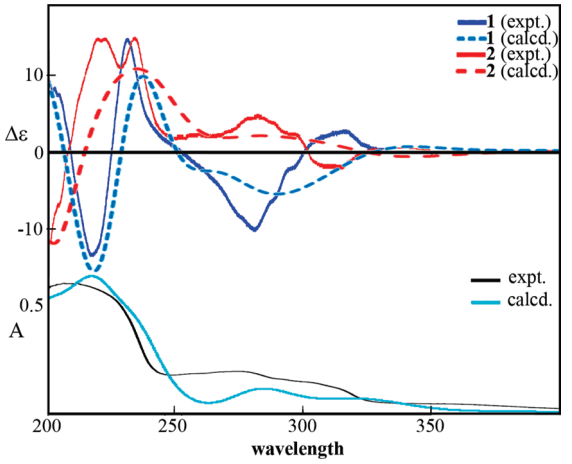

FIGURE 5. CD and UV spectra of bisnicalaterines B (**1**) and C (**2**). Dotted lines indicated simulated CD curves of **1** and **2**.

energy minima corresponding to the dihedral angles (135° for **1**; 305° for **2**) in bisnicalaterines B (**1**) and C (**2**) as shown in Figure 4. Each of the lowest energy conformers corresponding to bisnicalaterines B and C are represented as shown in Figures 3 and 4, respectively (**1**, 71.22 kcal/mol; **2**, 78.17 kcal/mol). Global minima conformer corresponding to bisnicalaterine B (**1**) possessed a twist conformation, in which the ring current effect caused by the other indole ring affects the chemical shift of *N*-Me (C-22′), while the conformer corresponding to bisnicalaterine C (**2**) adopted an extended conformation (Figure 3). This result was consistent with the NOESY data and proton vicinal coupling constants obtained. Furthermore, the conformational change among these conformers could not be observed by molecular dynamics calculation. These computational simulations indicated that each of bisnicalaterines B and C took an atropisomeric relationship.

The absolute configuration of both bisnicalaterines B (**1**) and C (**2**) could be assigned by comparing their experimental CD spectra with the calculated CD spectra (CD calculations were performed by Turbomole 6.1[31] using RI-TD-DFT-BP86/aug-cc-pVDZ[26−29,32] level of theory on RI-DFT-BP86/SVP[26−30] optimized geometries). The CD spectrum of **1** showed different pattern from that of **2** (Figure 5). The calculated CD spectra of the isomers with 16*S*,20*R*,21*R*,4′*R*,3′*R*,15′*R*,19′*E* configurations show similar CD pattern compared to those of **1** and **2** as shown in Figure 5. Therefore, their absolute stereochemistries were proposed as shown in Figure 3.

The vasodilators are useful for treatment of cerebral vasospasm and hypertension and for improvement of peripheral

(26) Halgren, T. *J. Am. Chem. Soc.* **1990**, *112*, 4710–4723.
(27) Eickorn, K.; Treutler, O.; Ohm, H.; Haser, M.; Ahlrichs, R. *Chem. Phys. Lett.* **1995**, *240*, 283–289.
(28) Becke, A. D. *Phys. Rev. A* **1988**, *38*, 3098–3100.
(29) Perdew, J. P. *Phys. Rev. B* **1986**, *33*, 8822–8824.
(30) Schafer, A.; Horn, H.; Ahlrichs, R. *J. Chem. Phys.* **1992**, *97*, 2571–2577.
(31) TURBOMOLE V6.1 2009, a development of University of Karlsruhe and Forschungszentrum Karlsruhe GmbH, 1989−2007; TURBOMOLE GmbH, since 2007; available from http://www.turbomole.com.
(32) Weigend, F.; Kohn, A.; Hattig, C. *J. Chem. Phys.* **2002**, *116*, 3175–3183.

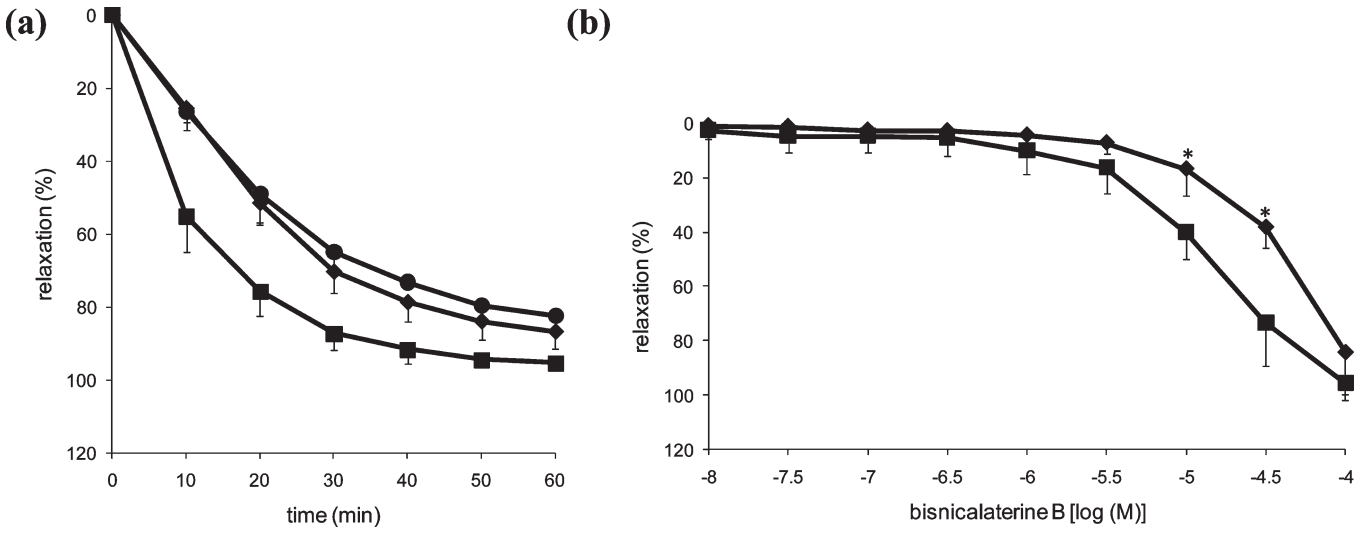

FIGURE 6. (a) Relaxation responses induced by bisnicalaterines B and C at 3×10^{-5} M in rat aortic rings precontracted with 3×10^{-7} M phenylephrine (PE) and effects of endothelium removal (−EC) on bisnicalaterine B-induced relaxation of PE-precontracted tone in isolated rat aorta rings. Symbols: ♦, bisnicalaterine B (+EC); ●, bisnicalaterine B (−EC); ■, bisnicalaterine C (+EC). Data are the means ± SD ($n = 3$). (b) Vasorelaxant Effects of bisnicalaterine B in endothelium-denuded aortic rings in the presence of 1 mM TEA. Symbols: ■, −EC; ♦, −EC TEA. Data are means ± SD ($n = 3$). *$P < 0.05$.

circulation. Several endothelium-dependent vasodilators, such as bradykinin, acetylcholine, and histamine, have been reported to elevate Ca^{2+} levels in endothelial cells and active NO release, leading to vasorelaxation.[19,20]

K^+ channels play important roles in the regulation of vascular tone.[21−23] Indeed, the K^+ channels present in blood vessels indirectly influence vascular tension by changing the resting membrane potential. By so doing, not only do they help to maintain the resting membrane potential of vascular smooth muscle, but they also modulate the relaxant/dilator response of blood vessel.[22,23] Many vascularly active agents and drugs induce their vasodilator or vasoconstrictor effects by opening or closing K^+ channels.[24]

The maximal relaxation of bisnicalaterine B, a major compound from *Hunteria zeylanica*, in endothelium-intact rings was 86.6 ± 4.9% (Figure 6a). In endothelium-denuded rings, the time course of bisnicalaterine B did not change significantly ($P > 0.05$ vs endothelium-intact group, $n = 3$), suggesting that the relaxant effect of bisnicalaterine B is endothelium-independent. Hence, subsequent investigations were focused on mechanisms of vasorelaxation that are independent of the endothelium. One such mechanism would be the opening of K^+ channels. To evaluate involvement of K^+ channels against vasorelaxant effect induced by bisnicalaterine B, we preincubated with a K^+ channel inhibitor [1 mM tetraethylammonium (TEA)].[25] The concentration−response curve for bisnicalaterine B was slightly shifted to the right after treatment with TEA. This suggested that bisnicalaterine B may activate vascular TEA-sensitive K^+ channels. As TEA does not abolish the relaxant response, activation of TEA-sensitive K^+ channels should account only partially for the relaxation induced by bisnicalaterine B. Further precise investigations on the vasorelaxant mechanism of bisnicalaterines are in progress.

Conclusions

In this work, two new bisindole alkaloids, bisnicalaterines B (**1**) and C (**2**), which exhibited potent vasorelaxant activity on isolated rat aorta, were isolated from the bark of *Hunteria zeylanica*. The structures and stereochemistry of **1** and **2** were elucidated and characterized by combination of NMR, CD, and computational methods, and each of them was shown to be atropisomeric relationship. Further investigation about SAR of bisnicalaterines is ongoing.

Experimental Section

General Methods. ^{1}H and 2D NMR chemical shifts were referenced to the residual solvent peaks (δ_H 3.31 and δ_C 49.0 for methanol-d_4). Standard pulse sequences were employed for the 2D NMR experiments. ^{1}H−^{1}H COSY, HOHAHA, and NOESY spectra were measured with spectral widths of both dimensions of 4800 Hz, and 32 scans with two dummy scans were accumulated into 1K data points for each of 256 t1 increments. NOESY spectra in the phase-sensitive mode were measured with a mixing time of 800 ms. For HMQC spectra in the phase-sensitive mode and HMBC spectra, a total of 256 increments of 1K data points were collected. For HMBC spectra with *Z*-axis PFG, a 50 ms delay time was used for long-range C−H coupling. Zero-filling to 1K for F1 and multiplication with squared cosine-bell windows shifted in both dimensions were performed prior to 2D Fourier transformation.

Material. Bark of *H. zeylanica* was collected in Kampung Padang, Malaysia, in 1994. The botanical identification was made by Mr. Teo Leong Eng, Faculty of Science, University of Malaya. A voucher specimen (Herbarium No. KL 4345) is deposited at the Herbarium of the Department of Chemistry, University of Malaya, Kuala Lumpur, Malaysia.

Extraction and Isolation. The bark of *H. zeylanica* was extracted with MeOH, and part (87 g) of the extract was treated with 3% tartaric acid (pH 2) and then partitioned with EtOAc. The aqueous layer was treated with saturated Na_2CO_3(aq) to pH 10 and extracted with $CHCl_3$ to give an alkaloidal fraction (5.33 g). The alkaloidal fraction was subjected to a Sephadex LH-20 column, and the fractions containing the dimer were further separated using amino silica gel column (*n*-hexane/EtOAc 9:1 → 2:8; $CHCl_3$/MeOH 9:1 → 0:1), followed by ODS SEPPAK (CH_3CN/H_2O 1:3 → 1:0) and ODS HPLC (H_2O/CH_3CN 71:29; TFA 0.1%) to give

bisnicalaterine B (**1**, 10 mg, 0.001%) and bisnicalaterine C (**2**, 7 mg, 0.0007%).

Bisnicalaterine B (1): yellowish amorphous solid; $[\alpha]^{20}_{D}$ −104 (*c* 1.0, MeOH); IR (KBr) ν_{max} 3430 cm^{-1}; UV (MeOH) λ_{max} 210 (ε 41000), 275 (13000), 295 (sh, 10000) and 360 (3000) nm; CD (MeOH) λ_{max} 209 (Δ 0), 219 (Δ −11.62), 226 (Δ 0), 233 (Δ 14.99), 254 (Δ 0), 282 (Δ −8.62), 300 (Δ 0), and 315 (Δ 4.47) nm; ^{1}H and ^{13}C NMR data, see Table 1; ESIMS *m*/*z* 605 $(M)^{+}$; HRESIMS *m*/*z* 605.3878 $[M^{+}]$ (calcd for $C_{39}H_{49}N_4O_2$, 605.3856).

Bisnicalaterine C (2): yellowish amorphous solid; $[\alpha]^{20}_{D}$ −159 (*c* 1.0, MeOH); IR (KBr) ν_{max} 3430 cm^{-1}; UV (MeOH) λ_{max} 210 (ε 29000), 275 (9000), 295 (sh, 7000) and 360 (2000) nm; CD (MeOH) λ_{max} 209 (Δ 0), 222 (Δ 14.62), 229 (Δ 11.12), 234 (Δ 14.99), 250 (Δ 1.96), 282 (Δ 4.83), 300 (Δ 0), and 314 (Δ −1.80) nm; ^{1}H and ^{13}C NMR data, see Table 1; ESIMS *m*/*z* 605 $(M)^{+}$; HRESIMS *m*/*z* 605.3814 $[M^{+}]$ (calcd for $C_{39}H_{49}N_4O_2$, 605.3856).

Conformational Analysis by Grid Search. The calculation was performed in Sybyl 7.2 using a grid search. The torsion angle on $N_1-C_{16}-C_{9'}-C_{10'}$ was varied from 0° to 355° in 5° increments to generate 72 unique conformers for grid search, covering the entire conformational space about this torsion bond. Energy minimization was performed on the conformers generated using MMFF94 force field[26] and charges.

Circular Dichroism Spectra Calculation. The conformations were obtained using Monte Carlo analysis with MMFF94 force field[26] and charges on Sybyl 7.2. Geometries were further optimized by using RI-*J*[27] approximation at the DFT BP86/SVP level of theory[28−30] in Turbomole 6.1.[31] Excited-state calculations were performed on the optimized ground state geometries at the RI-TD-DFT BP86/aug-cc-pVDZ[32] level of theory. The CD spectra were simulated by overlapping Gaussian functions for each transition where the width of the band at 1/*e* height is fixed at 0.3 eV, and the resulting spectra were scaled to the experimental values.

(33) Morita, H.; Iizuka, T.; Choo, C.-Y.; Chan, K.-L.; Takeya, K.; Kobayashi, J. *Bioorg. Med. Chem. Lett.* **2006**, *16*, 4609–4611.

Vasorelaxant Activity.[33] A male Wistar rat weighting 260 g was sacrificed by bleeding from carotid arteries under anesthesia. A section of the thoracic aorta between the aortic arch and the diaphragm was removed and placed in oxygenated, modified Krebs−Henseleit solution (KHS: 118.0 mM NaCl, 4.7 mM KCl, 25.0 mM $NaHCO_3$, 1.8 mM $CaCl_2$, 1.2 mM NaH_2PO_4, 1.2 mM $MgSO_4$, and 11.0 mM glucose). The aorta was cleaned of loosely adhering fat and connective tissue and cut into ring preparations 3 mm in length. The tissue was placed in a well-oxygenated (95% O_2, 5% CO_2) bath of 5 mL of KHS solution at 37 °C with one end connected to a tissue holder and the other to a force-displacement transducer (Nihon Kohden, TB-611T). The tissue was equilibrated for 60 min under a resting tension of 1.0 g. During this time, the KHS in the tissue bath was replaced every 20 min.

After equilibration, each aortic ring was contracted by treatment with 3×10^{-7} M phenylephrine (PE). The presence of functional endothelial cells was confirmed by demonstrating relaxation to 10^{-5} M acetylcholine (ACh), and aortic rings in which 80% relaxation occurred were regarded as tissues with endothelium. When the PE-induced contraction reached a plateau, each sample was added.

The animal experimental studies were conducted in accordance with the Guiding Principles for the Care and Use of Laboratory Animals, Hoshi University, and under the supervision of the Committee on Animal Research of Hoshi University, which is accredited by the Ministry of Education, Science, Sports Culture, and Technology of Japan.

Acknowledgment. This work was supported by a Grant-in-Aid for Scientific Research from the Ministry of Education, Culture, Sports, Science, and Technology of Japan, The Open Research Center Project, and Takeda Science Foundation.

Supporting Information Available: ^{1}H, ^{13}C, and 2D NMR spectra and atom coordinates of **1** and **2**. This material is available free of charge via the Internet at http://pubs.acs.org.